Supramolecular Chemistry
Publication details, including instructions for authors and subscription information:
http://www.informaworld.com/smpp/title~content=t713649759

Surface-Active Mononuclear and Dinuclear Ru(II) Complexes based on Thio-substituted Terpyridines Bearing Cyclodextrin Recognition Units

Maria José J. Pereira Silva[a]; Paolo Bertoncello[b]; Nikolaos N. Daskalakis[b]; Neil Spencer[a]; Benson M. Kariuki[a]; Patrick R. Unwin[b]; Z. Pikramenou[a]
[a] School of Chemistry, University of Birmingham, Edgbaston, UK [b] Department of Chemistry, University of Warwick, Coventry, UK

To cite this Article Silva, Maria José J. Pereira , Bertoncello, Paolo , Daskalakis, Nikolaos N. , Spencer, Neil , Kariuki, Benson M. , Unwin, Patrick R. and Pikramenou, Z.(2007) 'Surface-Active Mononuclear and Dinuclear Ru(II) Complexes based on Thio-substituted Terpyridines Bearing Cyclodextrin Recognition Units', Supramolecular Chemistry, 19: 1, 115 — 127
To link to this Article: DOI: 10.1080/10610270601026578
URL: http://dx.doi.org/10.1080/10610270601026578

Supramolecular Chemistry, January–March 2007 Vol. 19 (1–2), pp. 115–127

Taylor & Francis
Taylor & Francis Group

Surface-Active Mononuclear and Dinuclear Ru(II) Complexes based on Thio-substituted Terpyridines Bearing Cyclodextrin Recognition Units

MARIA JOSÉ J. PEREIRA SILVA[a], PAOLO BERTONCELLO[b], NIKOLAOS N. DASKALAKIS[b], NEIL SPENCER[a], BENSON M. KARIUKI[a], PATRICK R. UNWIN[b] and Z. PIKRAMENOU[a,*]

[a]*School of Chemistry, University of Birmingham, Edgbaston B15 2TT, UK;* [b]*Department of Chemistry, University of Warwick, Coventry CV4 7AL, UK*

(Received 15 June 2006; Accepted 29 August 2006)

Ruthenium(II) surface active complexes based on a tpySH ligand have been prepared and characterised, (1) [Ru(tpyada)(tpySH)]$(PF_6)_2$, (2) [Ru(biptpy)(tpySH)]$(PF_6)_2$ and (3) [Ru(pm-β-CD(ttp))(tpySH)]$(PF_6)_2$. The complexes bear a surface active thiol group and a recognition unit which is either a β-cyclodextrin or a hydrophobic tail (adamantyl- or biphenyl) in order to utilise cyclodextrin recognition for the formation of supramolecular wires using bottom up approaches. Monolayers of [Ru(tpyada)(tpySH)]$(PF_6)_2$ on ITO surfaces are studied by electrochemical techniques. Detailed NMR analysis of tpySH reveals the presence of two tautomers, an "NH" and an "SH" form. The X-ray crystal structure of the oxidised form of the ligand tpySStpy is reported. A new ligand tpySCH_2Stpy is prepared and its dinuclear Ru(II) complexes are reported, (4) [(ttp)Ru(tpyS CH_2 Stpy)Ru(ttp)]$^{+2}$, (5) [(biptpy)Ru(tpySCH_2Stpy)Ru (bitpy)]$^{+2}$, (6) [(pm-β-CD(ttp))Ru(tpySCH_2 Stpy)Ru(pm-β-CD(ttp))]$^{+2}$. The complexes show characteristic red ^{3}MLCT luminescence which is much stronger than their analogous mononuclear counterparts.

Keywords: Surface active metal complexes; Cyclodextrin; electrochemistry; Luminescence

INTRODUCTION

Attachment of polypyridyl metal complexes on surfaces is attractive for the formation of molecular wires based on the photochemical and electrochemical properties of the metal centres. Ruthenium(II) and osmium(II) tris(bipyridyl) complexes have been modified with thiol groups and their monolayers have been studied by surface, electrochemical techniques [1–5] and more recently by luminescence spectroscopy [5]. Moreover, a device based on nanostructured TiO_2 films with a functionalised Ru(II) tris(bipyridyl) complex covalently attached to a viologen unit has been used to demonstrate a write, read and erase process when incorporated in a sealed two-electrode cell [6].

To design linear arrays of metal complexes, terpyridine ligands provide the advantage of directionality control for building complexes from the surface [7]. The formation of self-assembled monolayers of Co, Cr and Os complexes on Au electrodes and their electrochemical characterization has been reported [8]. Co(II) thiol terpyridine complexes have also been considered as suitable single-molecule transistors [9,10]. The use of a pyridine surface anchoring group on terpyridines has led to formation of mono and dinuclear Ru(II) and Os(II) complexes [11].

We have been interested in the design of supramolecular wires based on metalloguests and metallocomplexes [12–15]. Metallocyclodextrins provide functional building blocks for supramolecular systems with a photoinduced function [16–19]. We have recently demonstrated that unidirectional energy transfer can take place in a solution assembled Ru(II) cyclodextrin junction [20,21]. In order to develop capability of forming supramolecular wires on surfaces, we have prepared thiol-active metalloguests and metallocomplexes. We also developed a new bis-terpyridine ligand that led to formation of interesting dinuclear ruthenium complexes.

*Corresponding author. E-mail: z.pikramenou@bham.ac.uk

ISSN 1061-0278 print/ISSN 1029-0478 online © 2007 Taylor & Francis
DOI: 10.1080/10610270601026578

RESULTS AND DISCUSSION

Synthesis and Characterisation of Thio-substituted 2,2′:6′,2″-Terpyridines

We have chosen to synthesize a tpySH ligand due to its versatility and one step synthesis (Scheme 1). The tpySH compound was synthesised using a modified method from the published procedure [9,22]. We found that the reaction was very sensitive to temperature, the quantity and quality (freshness) of $NaSCH_2CH_3$ leading to formation of $tpySCH_2Stpy$ (Scheme 2) which we now have independently synthesized and characterized. We have introduced an additional modification at the final step by treating the compound with hydrazine [23] since we found formation of the oxidized product tpySStpy (Scheme 2).

The ^{1}H NMR of tpySH was recorded in d_6-acetone and the characteristic resonances of a 4′ substituted terpyridine were present between 8.7–7.2 ppm (Supplementary Info). However, when the ^{1}H NMR of this compound was recorded in $CDCl_3$ a small set of peaks indicated the presence of a minor by-product. The peaks of the minor by-product increased in intensity with time (Supplementary Info). To examine the nature of the by-product a few drops of d_6-DMSO were added to a fresh solution of the compound in $CDCl_3$ and the NMR spectrum was recorded through the course of several days. It is well known that DMSO can act as an oxidizing agent for thiol groups producing the disulfide derivative [24,25]. After leaving the solution standing for 4 days, the ^{1}H NMR presented only one set of terpyridine resonances at a new set of chemical shifts, which showed a peak in ES-MS corresponding to the disulfide derivative, tpySStpy.

In order to elucidate the identity of the minor by-product present in a $CDCl_3$ solution, 1D GOESY studies were performed. In this experiment specific resonances of each one of the sets of terpyridine resonances were selectively excited and the nOe signals observed from the 1D GOESY experiment were examined. This was aimed at elucidating the possibility of the existence of two tautomeric forms in solution, "SH" and "NH" (Scheme 3). The selective excitation of the $H_{3'}$ resonance of the major product at 8.1 ppm yielded positive nOe

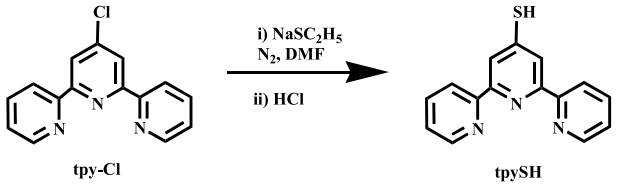

SCHEME 1

interactions with the resonances of H_3 and H_4 of the major product (blue labelling in Fig. 1). This indicates that $H_{3'}$ and H_3 are close in space and therefore the terpyridine may be in a structural arrangement where the outer pyridine rings are orientated with the nitrogen atoms pointing towards the terpyridine centre. In this experiment, a strong negative nOe signal at the $H_{3'}$ (8.62 ppm) resonance of the minor by-product (black labelling in Fig. 1) was also observed. The origin of such signal can be explained as saturation transfer from the selective excitation of the major product resonance. Due to the saturation of this resonance, a positive nOe signal is observed from the interaction of this $H_{3'}$ with H_3 of the same minor by-product. The fact that saturation transfer is observed under the conditions of the experiment indicates that: the two products are in slow interchange in relation to the NMR time scale explained with the two different sets of resonances observed for major and minor by-product; and there is interchange between the two products that happens faster than the experimental timescale so that saturation of the equivalent resonance in the minor terpyridine by-product is observed when selectively exciting $H_{3'}$ of the major product. From these observations we can tentatively assign the identities of the two products present in a $CDCl_3$ solution of tpySH ligand as corresponding to the two possible tautomeric forms of tpySH: "SH" and "NH" form (Scheme 3). In terms of electron density of each one of the tautomeric forms, and the effect over the $H_{3'}$ chemical shift, we could cautiously assign the major product in the NMR spectrum to the SH tautomer, and the NH tautomer to the minor by-product. We would expect the structure of the NH tautomer to have a larger deshielding effect over $H_{3'}$ than the SH tautomer.

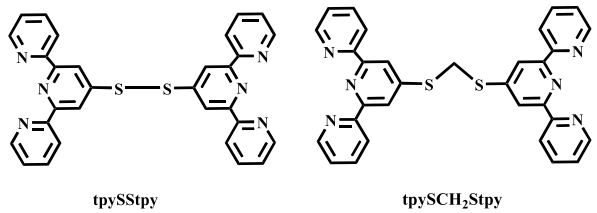

SCHEME 2

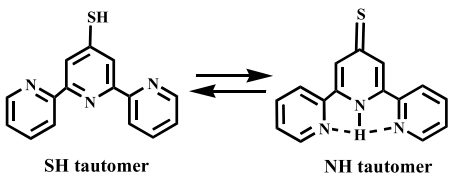

SCHEME 3

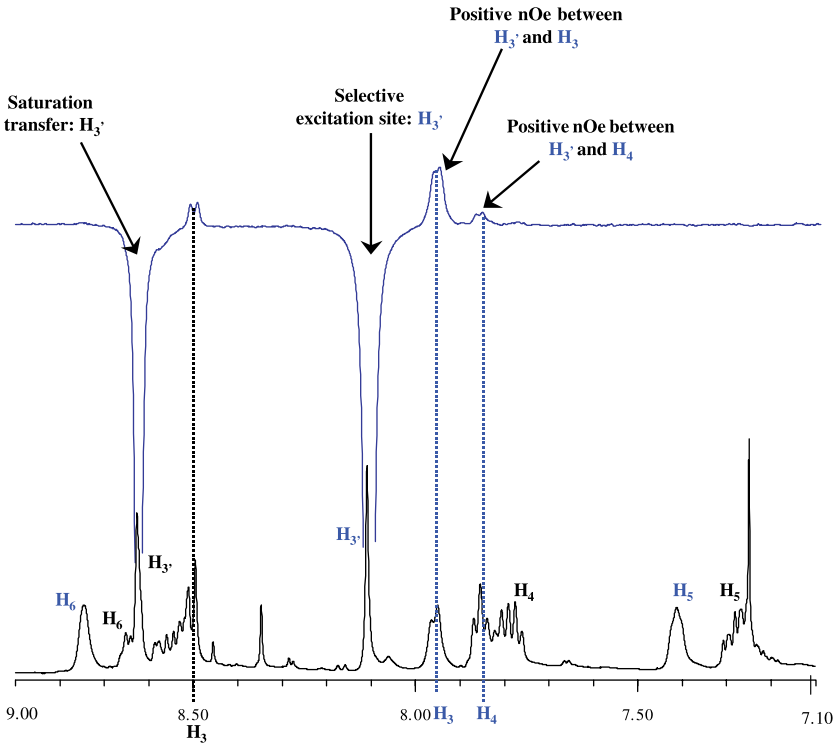

FIGURE 1 The 500 MHz 1D GOESY spectrum of tpySH in $CDCl_3$ with selective excitation of the $H_{3'}$ resonance at 8.11 ppm.

Similar deductions were made from the 1D GOESY spectrum recorded under the same conditions, but with selective excitation of the resonance of $H_{3'}$ at 8.62 ppm for the minor by-product (Supplementary Info). In this case when exciting $H_{3'}$ there was also excitation of the H_6 resonance (black labelling) due to overlapping of the two resonances. Positive nOe's signals towards H_3 and H_5 confirm the NH configuration, while the saturation transfer to $H_{3'}$ and H_6 of the blue labelled terpyridine system confirms the fast exchange between the two tautomeric forms of the major and minor product.

In conclusion, the results provide evidence that the compound tpySH in a $CDCl_3$ solution may exist in the two tautomeric forms: SH and NH. From the relative integration of the NMR resonances it was determined that the two tautomeric forms existed in solution in the ratio 3:2 of "SH" to "NH" forms. To further support our deductions, the shift of terpyridine protons were compared with the resonances of a model compound of the thiol tautomer, tpy-SCH_3, that effectively locks the molecular structure, thereby excluding any possibility of tautomerism. The resonance of the $H_{3'}$ proton for tpy-SCH_3 appeared at 8.22 ppm in $CDCl_3$ [26]. This resonance is comparable to that observed for the major product in the $CDCl_3$ spectrum at 8.15 ppm that we tentatively assigned as belonging to the SH tautomer. The two tautomers were also present in d_7-DMF, where the N—H proton of the "N—H" form was observed at 12.5 ppm.

The presence of tautomeric forms is not unusual for this type of system. A similar case is 4-hydroxyterpyridine which exists in solution in two tautomeric forms, one being the enol terpyridine and the other the keto form [27]. It was found that the ratio of the two tautomeric forms was dependent on the polarity and the hydrogen-bonding nature of the solvent used. Similar results were found for pyridine-4-thiol; the compound exists in solution as a mixture of the thiol (SH) and the thione (NH) tautomeric forms [28].

Single crystals of the surface-active tpySH compound were obtained in the oxidised form, tpySStpy, from a chloroform solution. The structure determination data are presented in Table I. The asymmetric unit contains half a molecule and the terpyridine rings are in the *trans*, *trans* conformation in the complete molecule (Fig. 2). Crystal packing is shown in Fig. 3.

The sulfur–sulfur, S(1)–S(1′), bond length is 2.031(1) Å and the C(1)–S(1) bond length is 1.778(2) Å; these values are in the same range as those reported previously for disulfide and carbon–sulfur bonds respectively [29]. The pyridine rings of the terpyridine are almost coplanar as shown by the interplanar angles (Table II). The values obtained, indicate that the each terpyridine is almost planar. The two terpyridine groups in the molecule are

TABLE I Crystal structure data for tpySStpy

Formula	$C_{30}H_{20}N_6S_2$
Formula weight	528.64
Temperature/K	296(2)
Wavelength/Å	1.54178
Crystal system	Monoclinic
Space group	*P*2/*n*
a/Å	11.7585(8)
b/Å	5.5378(4)
c/Å	19.5665(13)
β/°	90.528(4)
Volume/Å^3	1274.04(15)
Z	2
D_{cal}/Mg/m^3	1.378
Absorption coefficient/mm^{-1}	2.149
Crystal size/mm^3	0.24 × 0.04 × 0.02
Reflections collected	7775
Independent reflections	2305
R(int)	0.0401
Parameters	172
Goodness-of-fit on F^2	1.039
R1 [$I > 2\sigma(I)$]	0.0403
wR2	0.0959

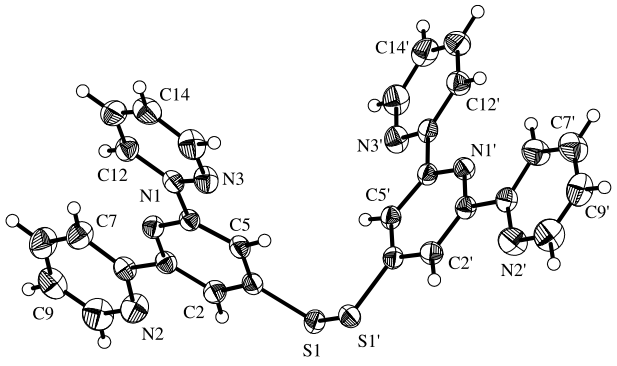

FIGURE 2 An ORTEP representation of the tpySStpy molecule.

almost perpendicular to each other and the torsion angle C(1)–S(1)–S(1′)–C(1′) is 91.273(3)°.

The tpySCH$_2$Stpy ligand was independently synthesized and characterized. The (+) ES MS spectra of tpySCH$_2$Stpy presented peaks for [M + H$^+$] and [M + Na$^+$] at m/z 543 and 565, respectively. Peaks for fragments corresponding to tpySCH$_2$ (m/z 278) and [tpyS + H$^+$] (m/z 265) were also observed. The ^{1}H NMR spectrum presented the characteristic terpyridine resonances in the aromatic region and at 4.84 ppm the resonance for the CH$_2$ protons of the thiol ether group. The assignments of the ^{1}H NMR and ^{13}C NMR spectra of tpySCH$_2$Stpy were confirmed by HSQC (Fig. 4). Cross-peaks were observed between the aromatic protons and the CH resonances in the ^{13}C NMR allowing the confirmation of the assignment presented above. The signal at 4.84 ppm presented a cross peak with a carbon resonance at 34 ppm confirming that the presence of a CH$_2$ group.

Synthesis of Mononuclear Surface-active Transition Metal Complexes

The surface-active ligands synthesized were used to generate transition metal complexes bearing one terpyridine with surface attachment function and one terpyridine with a cyclodextrin recognition site, such as adamantyl or biphenyl. The metal complex with an appended cyclodextrin was also prepared for surface attachment (Scheme 4).

We have used established routes for ruthenium terpyridine complexes to synthesize these surface-active metalloguests [30,31]. The complexes were characterised by (+) ES-MS, NMR and absorption spectroscopy. All spectra showed m/z signals for the loss of counter ions from the double charged species, although due to electrospray conditions they were

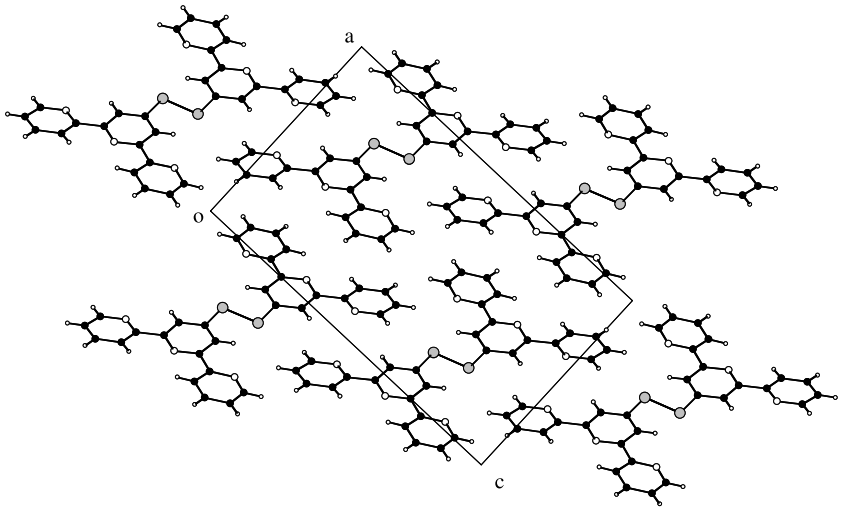

FIGURE 3 A view of the crystal structure down the b-axis tpySStpy.

TABLE II Interplanar angles (°) for planes a = N(1), C(1)–C(5), b = N(2), C(6)–C(10) and c = N(3), C(11)–C(15)

	a′	b	c
A	78.8	8.18	8.66
B		–	8.37

observed as monocharged peaks. The thiol group loses a proton, leaving the sulfur atom as S^-. This is not completely unexpected as the sulfur–proton bond is readily cleaved or exchanged [24]. The peaks observed showed the typical isotope patterns for mononuclear Ru(II) complexes. The ^{1}H NMR spectra have the characteristic resonances for 4′-substituted terpyridine-based heteroleptic complexes. These comprised of different resonant peaks for the protons on positions 3′ and 3, for both terpyridine units, along with an upfield shift to upfield of the H_6 and $H_{tpy\text{-}6}$ resonances in comparison with the uncomplexed ligand. A summary of the ^{1}H NMR resonances of the heteroleptic metalloguests, based on tpySH, is presented in Table III.

The UV-visible absorption spectrum of (1) in acetonitrile was recorded and showed the characteristic profile of a Ru(II) terpyridine complex. The high energy part of the spectrum is dominated by the ligand-based strong absorption bands due to $\pi-\pi^*$ transitions at 274 nm and 308 nm. The asymmetric broad absorption band encountered in the visible region of the spectrum, centred at 490 nm, is

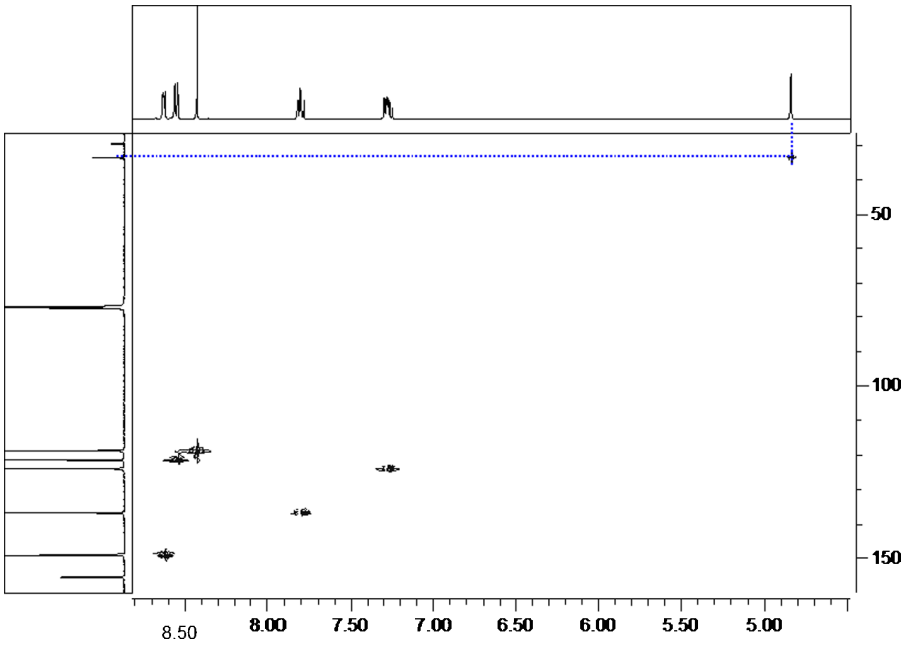

FIGURE 4 The 400 MHz gradient HSQC spectrum for tpySCH_2Stpy in $CDCl_3$.

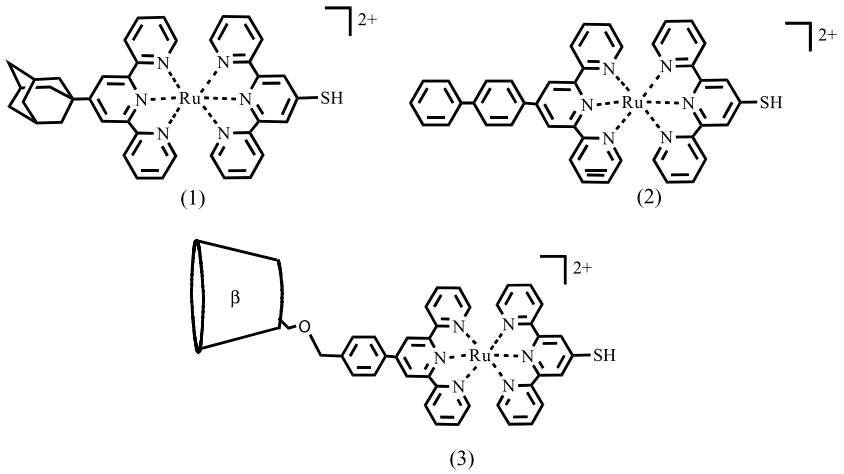

SCHEME 4

TABLE III ^{1}H NMR chemical shifts of (1), (2) and (3) in CD_3CN

	(**1**)	(**2**)	(**3**)
$H_{3'}/H_{tpy\text{-}3'}$ (s, 2H)	9.05	8.99	9.18
$H_{3'}/H_{tpy\text{-}3'}$ (s, 2H)	8.93	8.74	9.09
$H_3/H_{tpy\text{-}3}$ (d, 2H)	8.68 (8.7 Hz)	8.71 (8.2 Hz)	8.70 (8.1 Hz)
$H_3/H_{tpy\text{-}3}$ (d, 2H)	8.58 (8.4 Hz)	8.65 (7.5 Hz)	8.67 (8.4 Hz)
$H_{tpy\text{-}4}$, H_4 (m, 4H)	8.01–7.81	7.97–7.89	7.98–7.93
$H_{tpy\text{-}6}/H_6$ (d, 2H)	7.35 (5.4 Hz)	7.55 (6.5 Hz)	7.49 (6.9 Hz)
$H_{tpy\text{-}6}/H_6$ (d, 2H)	7.29 (4.2 Hz)	7.44 (5.7 Hz)	7.49 (6.9 Hz)
$H_{tpy\text{-}5}$, H_5 (m, 4H)	7.21–7.14	7.21–7.16	7.29–7.19
H_a/H_b (d, 2H)	–	8.19 (8.0 Hz)	8.34 (8.4 Hz)
H_a/H_b (d, 2H)	–	7.90 (8.2 Hz)	8.06 (8.1 Hz)
H_o (2H)	–	–	7.86 (7.2 Hz)
H_m, H_p (m, 3H)	–	–	7.58
H_c, H_d (br s, 9H)	2.30	–	–
H_e (br s, 6H)	1.97	–	–
$H_{CD\text{-}1}$ (br s, 7H)	–	5.12	–
$H_{CD\text{-}(2\text{-}6)}$	–	3.77–3.07	–

attributed to the spin allowed ^{1}MLCT. The ^{1}MLCT is red-shifted by 10 nm when compared with the spectrum in the same solvent for the homoleptic $[Ru(tpyada)_2](PF_6)_2$ ($\lambda_{MLCT} = 480$ nm). This could be explained by the electron-withdrawing properties of the thiol group in the 4′ position of the terpyridine, stabilising the ^{1}MLCT excited state [30].

Synthesis of the Ru(II) Dinuclear Complexes

The Ru(II) complexes were synthesised by reacting two equivalents of $[Ru(R\text{-}tpy)]Cl_3$ with the *bis*-terpyridine ligand, $tpySCH_2Stpy$ (Scheme 5). ES-MS spectra for the Ru(II) dinuclear complexes were recorded and showed the characteristic m/z signals for the loss of counter ions. The complexes showed m/z signals corresponding to the doubly and triply-charged species. The NMR spectra of the complexes revealed symmetry around the central sulfur bridge. The ^{1}H NMR spectrum of (**4**) showed resonances characteristic for a heteroleptic metal complex based on 4′-substituted terpyridines. The expected ^{1}H NMR shifts of 4′-substituted terpyridines upon complexation with Ru(II) were present: H_6 and $H_{tpy\text{-}6}$ peaks at 7.49 ppm and 7.44 ppm showed an upfield shift upon metal complexation. The presence of two resonant signals at 8.99 ppm and 8.90 ppm, for the $H_{3'}$ and $H_{tpy\text{-}3'}$ protons, indicated that the terpyridines have different substituents. The same effect was also observed for protons on positions 3 and 6, which presented different chemical shifts for the two terpyridines. The resonance for H_3 and $H_{tpy\text{-}3}$ appeared as two partially overlapped doublets at 8.67 ppm and 8.65 ppm. The singlet, assigned to the CH_3 resonance at 2.53 ppm, and the $S–CH_2–S$ singlet at 5.65 ppm, dominated the aliphatic region of the spectrum. The relative integration of the resonances in the aromatic region with the central CH_2 was 2:1, indicating symmetry around the CH_2 group. The CH_2 resonance was shifted downfield by 0.8 ppm in comparison with uncomplexed $tpySCH_2Stpy$ (4.84 ppm). The introduction of a positive charge with the metal centre induces the deshielding of these protons by alteration of the electronic environment around the sulfur atom. The assignments were confirmed by HSQC spectroscopy, particularly in assigning the CH_2 resonance for the dinuclear complexes.

The ^{1}H NMR resonances for the synthesized dinuclear Ru(II) complexes are summarised in Table IV.

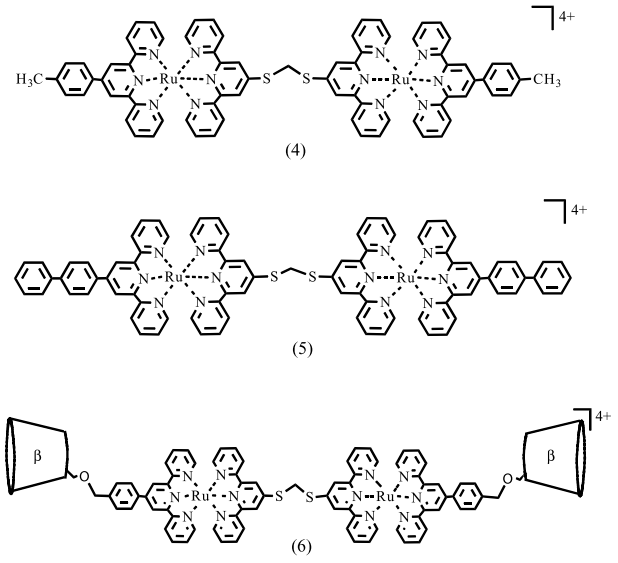

SCHEME 5

Photophysical Properties of the Ru(II) Dinuclear Complexes

The UV-visible absorption spectrum of (**4**) showed the $\pi-\pi^*$ ligand centred absorption bands at 287 nm and 307 nm and the MLCT band at $\lambda = 494$ nm. Upon excitation of the ^{1}MLCT, luminescence from

TABLE IV ^{1}H NMR chemical shifts of the dinuclear Ru(II) complexes of $tpySCH_2Stpy$ in CD_3CN

	(**4**)	(**5**)	(**6**)
$H_{3'}/H_{tpy\text{-}3'}$ (s, 4H)	9.00	8.99	9.29
$H_{3'}/H_{tpy\text{-}3'}$ (s, 4H)	8.92	8.90	9.09
$H_3/H_{tpy\text{-}3}$ (d, 4H)	8.66 (8.1 Hz)	8.67 (8.4 Hz)	8.99 (7.8 Hz)
$H_3/H_{tpy\text{-}3}$ (d, 4H)	–	8.65 (7.8 Hz)	8.69 (8.1 Hz)
$H_{tpy\text{-}4}$, H_4 (m, 8H)	7.97–7.93	7.97–7.89	7.97–7.89
$H_{tpy\text{-}6}/H_6$ (d, 4H)	7.50–7.43	7.49 (6.0 Hz)	7.50 (6.9 Hz)
$H_{tpy\text{-}6}/H_6$ (d, 4H)	–	7.44 (5.6 Hz)	7.45 (4.5 Hz)
$H_{tpy\text{-}5}$, H_5 (m, 8H)	7.25–7.17	7.23–7.16	7.24–7.16
H_a/H_b (d, 4H)	8.20 (8.1 Hz)	8.11 (8.4 Hz)	8.33 (8.4 Hz)
H_a/H_b (d, 4H)	7.74 (7.8 Hz)	7.58 (8.0 Hz)	8.06 (8.7 Hz)
H_o (4H)	–	–	7.86 (7.2 Hz)
H_m, H_p (t, 6H)	–	–	7.58 (7.2 Hz)
H_c, H_d (br s, 18H)	–	–	–
H_e (br s, 12H)	–	–	–
$H_{CD\text{-}1}$ (br s, 14H)	5.20	–	–
$H_{CD\text{-}(2\text{-}6)}$	3.82–3.08	–	–
$S–CH_2–S$	4.73	5.65	6.06

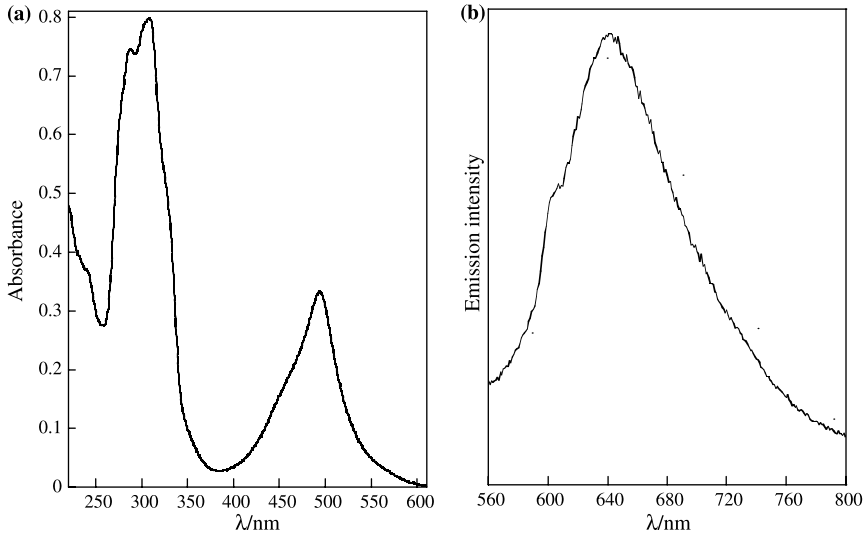

FIGURE 5 (a) UV–visible absorption and (b) emission spectra of (**4**) $\lambda_{exc} = 470\,nm$. The emission spectrum is corrected for the PMT response. Both spectra were recorded in acetonitrile solution.

the ^{3}MLCT was observed at $\lambda_{ems} = 638\,nm$ (Fig. 5). The luminescence relative quantum yield in acetonitrile was determined to be 2.0×10^{-4}, which is about six times larger than the value of 3.2×10^{-5} reported [30] for $[Ru(ttp)_2]^{+2}$.

The photophysical properties of (**5**) were investigated. The UV region of the spectrum presented strong absorbance bands arising from the $\pi-\pi^*$ ligand based transitions centred at 287 nm and 310 nm. The visible region of the spectrum is dominated by the charge transfer band (^{1}MLCT) centred at 495 nm, $\varepsilon = 8.15 \times 10^4\,cm^{-1}\,M^{-1}$. The model mononuclear $[Ru(biptpy)_2]^{+2}$ complex has been reported to have ^{1}MLCT centred at 494 nm [32] with $\varepsilon = 4.5 \times 10^4\,cm^{-1}\,M^{-1}$, which is approximately half the value for the dinuclear complex.

Upon excitation at $\lambda_{exc} = 495\,nm$, luminescence was detected at 645 nm (Fig. 6). The maximum of the emission is slightly shifted to the red in comparison with that observed for (**4**). This is due to the increase in the π-accepting nature of the biptpy tail in comparison with the tolyl group of the previous complex [30]. The luminescence relative quantum yield for this complex in acetonitrile was measured as 1.5×10^{-4}.

Electrochemistry Studies for Ru(II) Thio-based Surface-Active Metalloguest

Monolayer of the complex (**1**) were formed on indium tin oxide (ITO) electrodes and studied by cyclic voltammetry. ITO proved to be the optimal

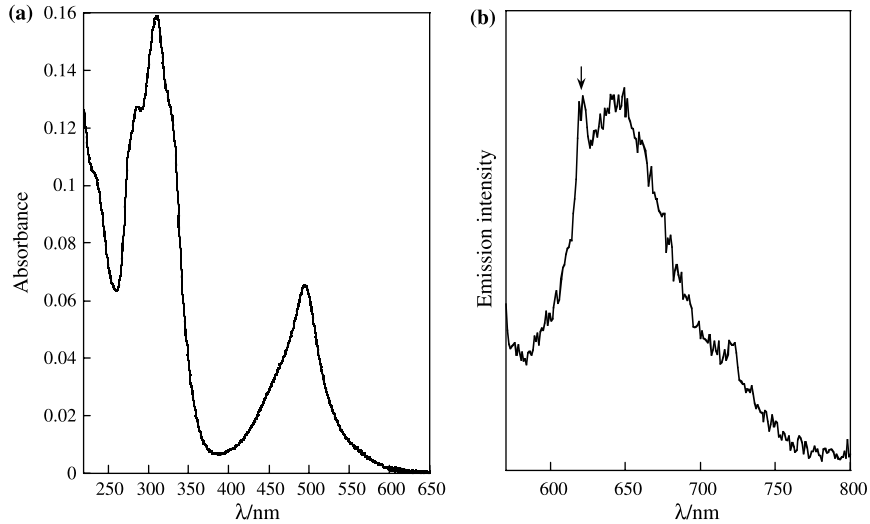

FIGURE 6 (a) UV-visible absorption and (b) emission spectra of (**5**), $\lambda_{exc} = 495\,nm$. The emission spectrum was corrected for PMT response. Both spectra were obtained for acetonitrile solutions of the complex. The peak indicated by the arrow is due to scattering.

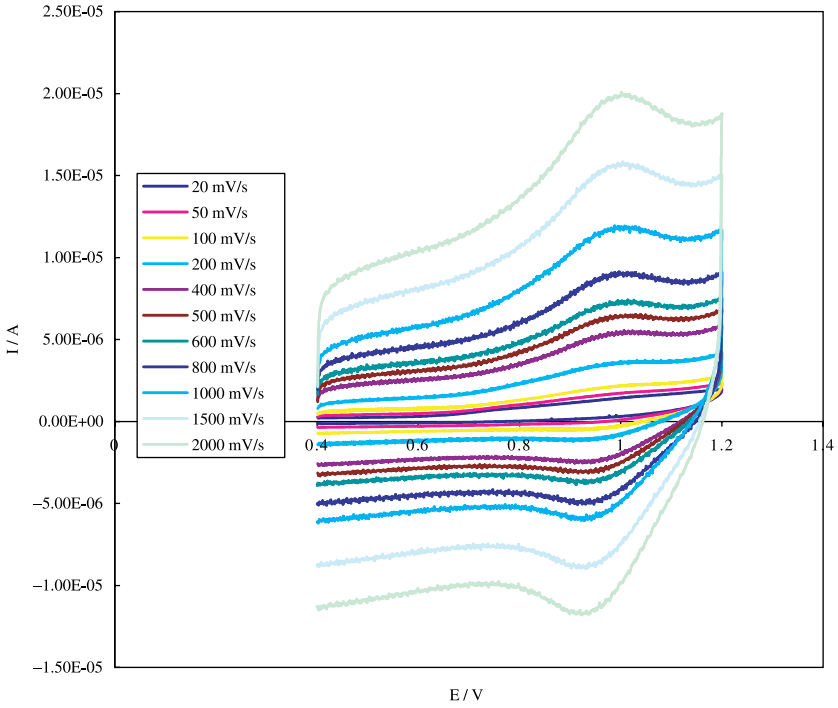

FIGURE 7 CVs of a [Ru(tpyada)(tpySH)]$(PF_6)_2$ SAM on an ITO electrode in acetonitrile, 0.1 M $TBAPF_6$ as supporting electrolyte at different scan rates.

surface for forming the monolayers, as evidenced by the most clean voltammetric responses. An ITO electrode with an area of 0.24 cm^2 was used to adsorb the Ru(II) sulfur based complex from solutions containing 2 mM of the complex in order to form monolayer. Voltammetric measurements of the films were carried out in anhydrous acetonitrile, and a clear reversible process was evident (Fig. 7). A well defined and reversible response was observed for all scan rates up to 2 V s^{-1}. The anodic peak for the oxidation of the Ru(II) complex occurred at *ca.* 1 V (*vs* Ag/Ag^+) whereas the reduction peak occurred at *ca.* 0.95 V: these values of the redox peaks are similar to those reported for $Ru(bpy)_3^{2+}$ [33]. The peak–peak separation ($\Delta E_p = E_p^f - E_p^b$, where E_p^f and E_p^b are the peak potentials for the forward and back scans) were found to be *ca.* 50 mV at $v = 500$ mV s^{-1} and increased with the scan rate. The fact the peak separation is lower than 59 mV is indicative of a contribution from a surface- confined species, indicating adsorption onto the surface [34]. The most striking evidence of a surface process is

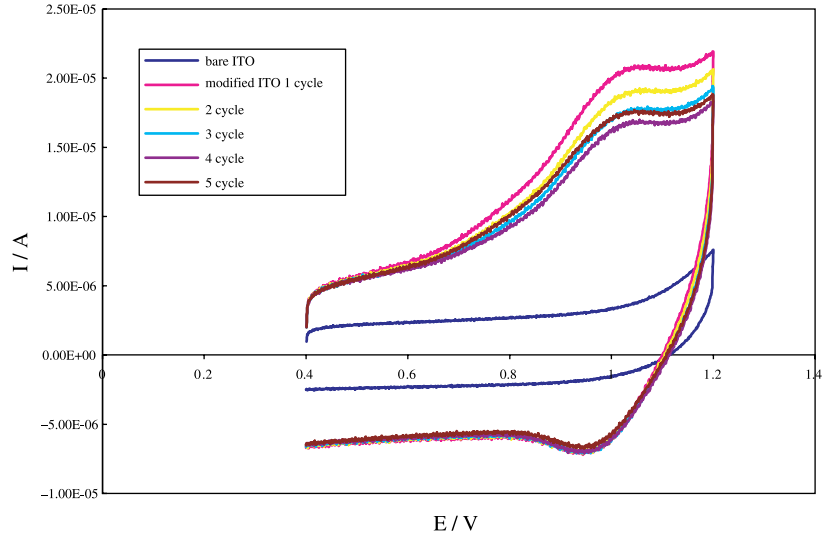

FIGURE 8 CVS of a [Ru(tpyada)(tpySH)]$(PF_6)_2$ SAM ($c = 2$ mM) on a ITO electrode in acetonitrile, 0.1 M $TBAPF_6$ as supporting electrolyte with continuous cycling at 1 V s^{-1}.

TABLE V Variation of the charge and surface coverage with increase number of cycles

Cycle number	Charge/10^{-7} (C)	$\Gamma/10^{-11}$ (mol cm^{-2})
1	9.36	4.04
2	8.83	3.81
3	8.43	3.64
4	8.12	3.51
5	7.96	3.44
6	7.45	3.22

that the peak current scales linearly with scan rate. As experiments were carried out in a solution that did not contain the complex, there is no contribution to the current from diffusive process [34]. The stability of the monolayer under these conditions was investigated further, as reported below.

Consecutives cycles at the same scan rate were performed and the change in the resulting CV was monitored. This experiment was performed for 50, 600 and 1000 mV s^{-1} scan rates. Similar observations were made for the three sets of independent experiments and, as an example, the results obtained for the 1000 mV s^{-1} scan rate are considered (Fig. 8). In this case, it is clear that the CV response is highly reversible over time, but that there is a small decrease in the peak current, with each scan. By integrating $i - V$ characteristics, the charge and surface coverage can be obtained (Table V).

The decrease observed in surface coverage with increase number of cycles is indicative of some loss of electroactive species adsorbed in the ITO electrode. Nonetheless, the surface coverages for these large complexes are reasonable and it is clear that [Ru(tpyada)(tpySH)]$(PF_6)_2$ electroactive SAMs can be formed on an ITO electrode surface.

CONCLUSIONS

We have prepared Ru(II) surface active complexes with appended guest and host moieties for the development of supramolecular wires on surfaces and examined the electrochemical properties of a Ru(II) surface active guest. Monolayers of the complex show promising electrochemical behaviour. The tpySH ligand proved a versatile motif for surface attachment and we have explored the tautomerism properties that may affect its surface binding studies. A ligand for dinuclear complexes was prepared and the dinuclear Ru(II) complexes were investigated. The complexes show interesting photophysical properties which may lead to further studies in solution assembly of metallocyclodextrins-metalloguests.

Supplementary material includes NMR spectra. Crystallographic data are deposited at the Cambridge Crystallographic Data Centre CDC 611415.

EXPERIMENTAL

Materials and Instrumentation

All starting materials were purchased from Aldrich unless otherwise indicated. Solvents used in synthetic procedures were analytical grade with the exception of HPLC grade solvents used in spectroscopic studies. Double deionised water was used where necessary in the spectroscopic studies. All the ligand synthetic procedures were carried out under nitrogen atmosphere. Thin layer chromatography (TLC) analyses were performed on either Merck silica gel 60 aluminium plates or Merck alumina Brockman I grade, as indicated. $RuCl_3{\cdot}3H_2O$ was kindly supplied from Johnson & Matthey.

The synthesis of 4′-(1-adamantyl)-2,2′: 6′,2″-terpyridine (tpyada), 4′-tolyl-2,2′: 6′,2″-terpyridine (ttp) and 4′-(4-biphenyl)-2,2′: 6′,2″-terpyridine (biptpy), pm-β-CD(ttp) were prepared by published methods.REF

NMR spectra were recorded on Bruker AC 300, AV 300 and DRX 500. Electrospray mass spectra were recorded on a Micromass LC-TOF machine. Elemental analyses were recorded on a Carlo Erba EA1110 simultaneous CHNS elemental analyser at the University of Birmingham.

Single Crystal X-Ray diffraction data was collected at 296 K on a Brüker Smart 6000 diffractometer equipped with a CCD detector and a copper tube source. Structures were solved and refined using SHELXL [35]. Absorption spectra were recorded on a Shimadzu UV-3101PC UV–Vis-NIR scanning spectrometer. Emission spectra were recorded on a Photon Technology International QM-1 steady state spectrometer employed with a dual grating 500/750 nm emission monochromator. Quantum yields were determined using the "optical dilute relative method" [36] using $[Ru(2,2'\text{-bipyridyl})_3]Cl_2$ as a reference with $\Phi = 0.028$ in aerated H_2O [37]. The GOESY or one-dimensional gradient NOE spectroscopy spectrum was recorded at 27°C using a Bruker DRX 500 with 7 seconds relaxation delay and 5 Hz of selective excitation. Each spectrum was obtained as accumulation of 512 scans.

Formation of Self-Assembled Monolayers (SAMs)

Spontaneously adsorbed monolayers were formed upon immersion of the ITO electrode in solutions of the complex in acetonitrile at the concentrations between 1–5 mM for 24 hours. Before electrochemical measurements were made, the electrodes were rinsed with acetonitrile in order to remove any unbound material. Subsequent measurements were performed in blank electrolyte containing 0.1 M $TBAPF_6$ as supporting electrolyte.

Electrochemistry

Cyclic voltammograms were recorded using an electrochemical analyzer (CH Instruments, model CHI730A). A typical three electrode configuration was used, where the working electrode was an ITO coated glass plate on which the SAM film was deposited, a platinum coil was used as counter electrode. Potentials are all referenced against a nonaqueous Ag/Ag^+ reference containing 5×10^{-3} M $Ag(NO_3)$ The area of the working electrode was kept constant (typically between 0.2–0.3 cm^2) during all measurements.

The surface coverage calculated is based on the measurement of Q, the charge passed to electrolyze the electroactive sites. A definition of Γ is given by the equation:

$$\Gamma = \frac{Q}{nFA}$$

where n is the number of electrons transferred; F is the Faraday's constant and A is the electrode area.

4′-(Mercapto)-2,2′: 6′,2″-Terpyridine (tpySH)

A solution of tpy-Cl (1.01 g; 3.78 mmol) and $NaSCH_2CH_3$, 90% pure (1.64 g; 1.95 mmol) in dry DMF (20 mL) was heated to 150°C in a silicone oil bath for 6 hours. A mixture of a yellow solution with a white solid was obtained. The reaction was filtered and after evaporation of the filtrate a yellow solid was obtained. The yellow solid was redissolved in acetone that upon evaporation yielded an oil. Upon addition of ether the precipitation of an off-white solid was achieved and was collected by filtration and washed with ether yielding 0.20 g (20%). The solid was treated with hydrazine monohydrate (0.5 mL) in a methanol/pyridine (1:1) solution to produce the free thiol ligand.

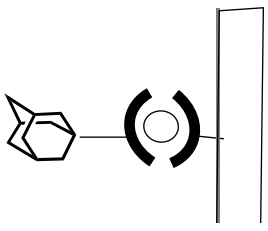

^{1}H-NMR (300 MHz, $(CD_3)_2CO$): δ in ppm 8.63 (d, 2H, H_6, $J = 5.7$ Hz); 8.28 (d, 2H, H_3, $J = 8.1$ Hz); 8.16 (s, 2H, $H_{3'}$); 7.89 (td, 2H, H_4, $J = 7.5$ Hz, $J = 1.8$ Hz); 7.32 (ddd, 2H, H_5, $J = 7.5$ Hz, $J = 4.8$ Hz, $J = 1.2$ Hz). ^{13}C NMR (75 MHz, CD_3Cl): δ in ppm 156, 155, 149.7, 146.7, 138, 126, 121, 117.

ES-MS (+) m/z: 288 $[M + Na]^+$; 266 $[M + H]^+$. Anal. Found: C, 67.94; H, 4.16; N, 15.82. Calcd for ($C_{15}H_{11}N_3S$): C, 67.90; H, 4.18; N, 15.84. UV–Vis in CH_3OH: λ_{max} in nm (ε in $M^{-1}\,cm^{-1}$) 280 (20190); 300 (17550); 312 (15160); 386 (8645).

bis(4′-(Mercapto)-2,2′: 6′,2″-terpyridyl)methane (tpySCH$_2$Stpy)

In a two neck flask tpy-Cl (0.55 g, 2.06 mmol) and an excess of $NaSCH_2CH_3$ (0.87 g; 10.3 mmol) were added. After the addition of 15 mL of dry DMF a yellow suspension was formed. The solution was refluxed for 30 hours with the aid of a heating mantel. The solution colour changed to dark orange. The solvent volume was reduced to one third and 50 mL of 0.1 N HCl were added precipitating an off white solid. The solid was collected by suction filtration and then redissolved in $CHCl_3$ and washed with water (3 × 30 mL). The combined organic layers were dried over anhydrous $NaSO_4$ followed by filtration. Evaporation of the solvent lead to 0.23 g of the product tpySCH_2Stpy (25%). ^{1}H-NMR (400 MHz, CD_3Cl): δ in ppm 8.63 (d, 4H, H_6, $J = 4.8$ Hz); 8.55 (d, 4H, H_3, $J = 8.0$ Hz); 8.43 (s, 4H, $H_{3'}$); 7.80 (td, 4H, H_4, $J = 7.6$ Hz, $J = 1.6$ Hz); 7.30–7.26 (m, 4H, H_5); 4.84 (s, 2H, S–CH_2–S).

^{13}C NMR (100 MHz, $CDCl_3$): δ in ppm 155.6, 155.3, 149, 148.8, 136.7, 123.8, 121.3, 118.7, 33.6 ES-MS (+) m/z: 543 $[M + H]^+$.

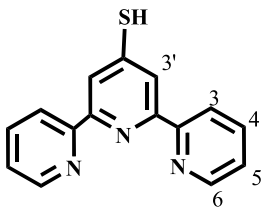

(1) [Ru(tpyada)(tpySH)](PF$_6$)$_2$

A solution of Ru(tpyada)Cl_3 (0.081 g; 0.141 mmol) and tpySH (0.041 g; 0.142 mmol) in 20 mL of methanol was refluxed in the dark for 24 hours. After cooling down to room temperature a solution of NH_4PF_6 in methanol was added to the reaction and a dark solid precipitated out. The solid was collected by filtration and washed with methanol and diethyl ether giving 0.093 g of the product (67%). ^{1}H-NMR (300 MHz, CD_3CN): δ in ppm 9.05 (s, 2H, $H_{3'/tpy\text{-}3'}$); 8.93 (s, 2H, $H_{3'/tpy\text{-}3'}$); 8.68 (d, 2H, $H_{3/tpy\text{-}3}$, $J = 8.7$ Hz); 8.58 (d, 2H, $H_{3/tpy\text{-}3}$, $J = 8.4$ Hz); 8.01–7.81 (m, 4H, H_4, $H_{tpy\text{-}4}$); 7.35

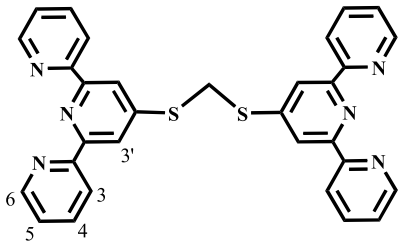

(d, 2H, $H_{6/tpy\text{-}6}$, $J = 5.4$ Hz); 7.29 (d, 2H, $H_{6/tpy\text{-}6}$, $J = 4.2$ Hz); 7.21–7.14 (m, 4H, H_5, $H_{tpy\text{-}5}$); 2.30 (br s, 9H, H_c,H_d); 1.97 (br s, 6H, H_e). ES-MS (+) m/z: 733 [M-$2PF_6$]$^+$ UV–Vis in CH_3CN: λ_{max} in nm (ε in $M^{-1}\,cm^{-1}$) 237; 276; 308; 492.

(2) [Ru(biptpy)(tpySH)](PF$_6$)$_2$

The complex was synthesised using the method described previously for [Ru(tpyada)(tpySH)]$(PF_6)_2$ starting with [Ru(biptpy)]Cl_3 (0.150 g; 0.254 mmol) and tpySH (0.199 g; 0.70 mmol). A methanolic solution of NH_4PF_6 was added to the reaction and a solid precipitated. The solid was collected by filtration and was purified by silica chromatography (eluents: CH_3CN followed by $CH_3CN/H_2O/KNO_3$ (sat) (70:0.5:1.5)). The counterion of the product was changed with a methanolic solution of NH_4PF_6 obtaining 0.010 g (43%) of the desired compound as a red solid.

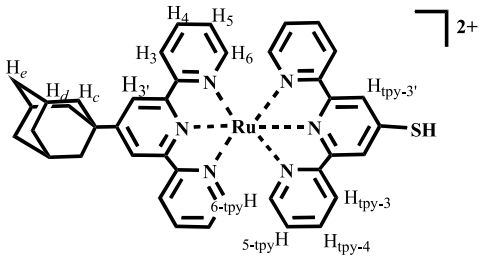

^{1}H-NMR (300 MHz, CD_3CN): δ in ppm 9.18 (s, 2H, $H_{3'/tpy\text{-}3'}$); 9.09 (s, 2H, $H_{3'/tpy\text{-}3'}$); 8.70 (d, 2H, $H_{3/tpy\text{-}3}$, $J = 8.1$ Hz); 8.67 (d, 2H, $H_{3/tpy\text{-}3}$, $J = 8.4$ Hz); 8.34 (d, 2H, $H_{a/b}$, $J = 8.4$ Hz); 8.06 (d, 2H, $H_{a/b}$, $J = 8.1$ Hz); 7.98–7.93 (m, 4H, H_4, $H_{tpy\text{-}4}$); 7.86 (d, 2H, H_o, $J = 7.2$ Hz); 7.58 (m, 3H, H_m, H_p); 7.49 (d, 4H, H_6, $H_{tpy\text{-}6}$, $J = 6.9$ Hz); 7.29–7.19 (m, 4H, H_5, $H_{tpy\text{-}5}$). ES-MS (+) m/z: 719 [M-$2PF_6$]$^+$; 359.5 [M-$2PF_6$]$^{+2}$.

(3) [Ru (pm-β-CD(ttp))(tpySH)](PF$_6$)$_2$

[Ru(pm-β-CD(ttp))]Cl_3 (0.046 g; 0.024 mmol) was dissolved in 5 mL of methanol with tpySH (0.017 g; 0.059 mmol) in the presence of a few drops of N-ethylmorpholine and refluxed for 24 hours. The reaction was allowed to cool down to room temperature and then filtered through celite. A methanolic solution of NH_4PF_6 was added to the filtrate and the solvent was evaporated. The residue

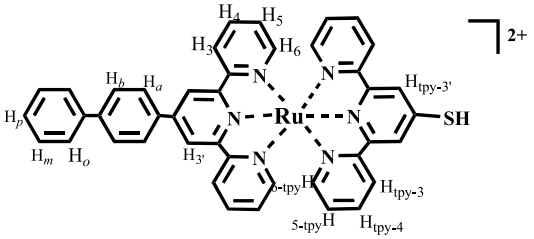

was extracted with CH_2Cl_2 and the insoluble solid was filtered out and the filtrate was evaporated yielding a red solid. The red residue was purified by size exclusion chromatography (BioBeads SX3) using DMF/THF (0.5:1). This solid was then stirred in a 1:1 mixture of methanol and pyridine with 0.3 mL of hydrazine monohydrate giving 0.047 g (80%) of the product as a red solid.

^{1}H-NMR (300 MHz, CD_3CN): δ in ppm 8.99 (s, 2H, $H_{3'/tpy\text{-}3'}$); 8.74 (s, 2H, $H_{3'/tpy\text{-}3'}$); 8.71 (d, 2H, $H_{3/tpy\text{-}3}$, $J = 8.2$ Hz); 8.65 (d, 2H, $H_{3/tpy\text{-}3}$, $J = 7.5$;Hz); 8.19 (d, 2H, $H_{a/b}$, $J = 8.0$ Hz); 7.97–7.89 (m, 4H, H_4, $H_{tpy\text{-}4}$); 7.90 (d, 2H, $H_{a/b}$, $J = 8.2$ Hz); 7.55 (d, 2H, $H_{6/tpy\text{-}6}$, $J = 6.5$ Hz); 7.44 (d, 2H, $H_{6/tpy\text{-}6}$, $J = 5.7$ Hz); 7.21–7.16 (m, 4H, H_5, $H_{tpy\text{-}5}$); 5.12 (br s, 7H, $H_{CD\text{-}1}$); 3.77–3.07 (m, $H_{CD\text{-}2,\ CD\text{-}3,\ CD\text{-}4,\ CD\text{-}5,\ CD\text{-}6}$, CD_{CH3}) ES-MS (+) m/z: 2102 [M − $2PF_6$]$^+$.

(4) [(ttp)Ru(tpySCH$_2$Stpy)Ru(ttp)](PF$_6$)$_4$

A suspension of $tpySCH_2Stpy$ (0.029 g; 0.069 mmol) and Ru(ttp)Cl_3 (0.069; 0.13 mmol) in 10 mL of methanol was prepared. A few drops of *N*-ethylmorpholine were added and the reaction was refluxed for 30 minutes. After cooling down to room temperature the solution was filtered through celite. A methanolic solution of NH_4PF_6 was added to the filtrate leading to precipitation of a dark red solid. The solid was collected by filtration and washed with methanol. The precipitate was purified by column chromatography on silica (eluent: $CH_3CN/H_2O/KNO_3$ (sat) (70:5:15)). The excess of KNO_3 was eliminated by adding NH_4PF_6 to a methanol solution of the fraction collected from the

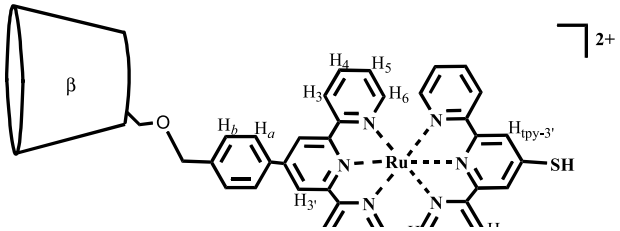

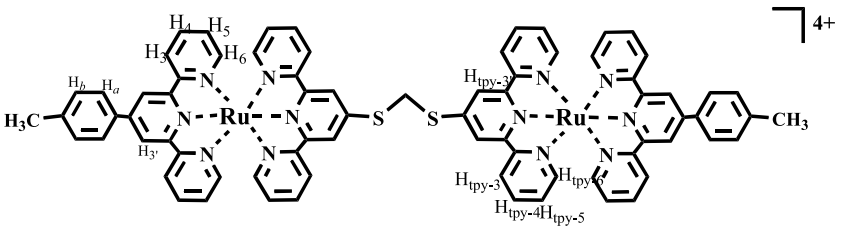

column yielding 0.08 g of the desired compound. Yield: 79%.

^{1}H-NMR (400 MHz, CD_3CN): δ in ppm 8.99 (s, 4H, $H_{3'/tpy\text{-}3'}$); 8.90 (s, 4H, $H_{3'/tpy\text{-}3'}$); 8.67 (d, 4H, $H_{3/tpy\text{-}3}$, $J = 8.4$ Hz); 8.65 (d, 4H, $H_{3/tpy\text{-}3}$, $J = 8.0$ Hz); 8.11 (d, 4H, $H_{a/b}$, $J = 8.4$ Hz); 7.97–7.89 (m, 8H, H_4, $H_{tpy\text{-}4}$); 7.58 (d, 4H, $H_{a/b}$, $J = 8.0$ Hz); 7.49 (d, 4H, $H_{6/tpy\text{-}6}$, $J = 6.0$ Hz); 7.44 (d, 4H, $H_{6/tpy\text{-}6}$, $J = 5.6$ Hz); 7.23–7.16 (m, 8H, H_5, $H_{tpy\text{-}5}$); 5.65 (s, 2H, S–CH_2–S); 2.53 (s, 6H, CH_3).

^{13}C NMR (100 MHz, CD_3CN): δ in ppm 159.3, 158.8, 156.5, 156, 153.6, 153.5, 149.4, 148.3, 142, 139, 134.9, 131.3, 128.6, 128.5, 125.8, 125.5, 122.6, 122.4, 35.1, 21.3. ES-MS (+) m/z: 841 $[M\text{-}2PF_6]^{+2}$; 512 $[M\text{-}3PF_6]^{+3}$. UV–Vis in CH_3CN: λ_{max} in nm (ε in $M^{-1}\,cm^{-1}$) 287 (144120); 307 (154560); 494 (64980).

[(pm-β-CD(ttp))Ru(tpySCH$_2$Stpy)Ru(pm-β-CD(ttp))](PF$_6$)$_4$

A solution of [Ru(pm-β-CD(ttp))]Cl_3 (0.101 g; 0.052 mmol) was refluxed with tpySCH_2Stpy (0.014 g; 0.033 mmol) in 10 mL of methanol with a few drops of N-ethylmorpholine for 24 hours. After cooling down to room temperature the reaction was

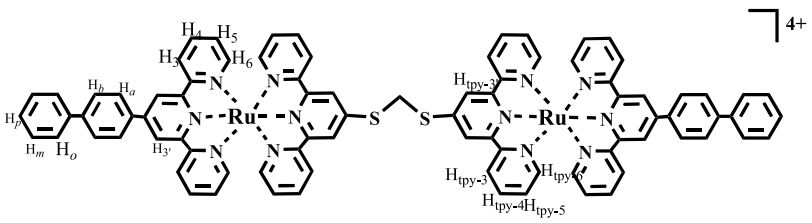

(5) [(biptpy)Ru(tpySCH$_2$Stpy)Ru(biptpy)](PF$_6$)$_4$

The complex [(biptpy)Ru(tpySCH_2Stpy)Ru(biptpy)]$(PF_6)_4$ was synthesised using the same method described previously for [(ttpRu(tpySCH_2-Stpy)Ru(ttp)]$(PF_6)_4$ starting with 0.049 g (0.084 mmol) of [Ru(biptpy)]Cl_3 and 0.022 g (0.053 mmol) of tpySCH_2Stpy in 5 mL of methanol with a few drops of *N*-ethylmorpholine. The product was obtained as 0.082 g of a dark red solid with a yield of 93%.

^{1}H-NMR (300 MHz, CD_3CN): δ in ppm 9.29 (s, 4H, $H_{3'/tpy\text{-}3'}$); 9.09 (s, 4H, $H_{3'/tpy\text{-}3'}$); 8.99 (d, 4H, $H_{3/tpy\text{-}3}$, $J = 8$ Hz); 8.69 (d, 4H, $H_{3/tpy\text{-}3}$, $J = 8$ Hz); 8.33 (d, 4H, $H_{a/b}$, $J = 8.5$ Hz); 8.06 (d, 4H, $H_{a/b}$, $J = 8.5$ Hz); 7.99–7.89 (m, 8H, H_4, $H_{tpy\text{-}4}$); 7.86 (d, 4H, H_o, $J = 7$ Hz); 7.58 (t, 6H, H_m, H_p, $J = 7$ Hz); 7.50 (d, 4H, $H_{6/tpy\text{-}6}$, $J = 7$ Hz); 7.45 (d, 4H, $H_{6/tpy\text{-}6}$, $J = 4.5$ Hz); 7.24–7.16 (m, 8H, H_5, $H_{tpy\text{-}5}$); 6.06 (s, 2H, S–CH_2–S). ^{13}C NMR (75 MHz, CD_3CN): δ in ppm 159, 153.5, 153.3, 148.6, 144, 138.9, 136.6, 130.1, 129.2, 128.9, 128.4, 128, 126, 125.4, 123, 122.4, 31.5. ES-MS (+) m/z: 903 $[M - 2PF_6]^{+2}$; 553 $[M - 3PF_6]^{+3}$. Anal. Found: C, 48.81; H, 3.07; N, 7.76. Calcd for ($C_{85}H_{60}N_{12}Ru_2S_2$ $(PF_6)_4$): C, 48.72; H, 2.89; N, 8.02. UV–Vis in CH_3CN: λ_{max} in nm (ε in $M^{-1}\,cm^{-1}$) 230(sh) (123450); 287 (158340); 309 (196870); 327(sh) (157390); 495 (81350).

filtered through celite and a methanolic solution of NH_4PF_6 was added to the filtrate. The solvent was evaporated and the residue was extracted with CH_2Cl_2. The mixture was filtered and the filtrate was evaporated yielding a red solid. The red residue was purified by size exclusion chromatography BioBeads SX3 using DMF/THF (1:1) yielding 0.064 g (55%) of the product.

^{1}H-NMR (300 MHz, CD_3CN): δ in ppm 9.00 (s, 4H, $H_{3'/tpy\text{-}3'}$); 8.92 (s, 4H, $H_{3'/tpy\text{-}3'}$); 8.66 (d, 8H, H_3, $H_{tpy\text{-}3}$, $J = 8.1$ Hz); 8.20 (d, 4H, $H_{a/b}$, $J = 8.1$ Hz); 7.97–7.93 (m, 8H, H_4, $H_{tpy\text{-}4}$); 7.74 (d, 4H, $H_{a/b}$, $J = 7.8$ Hz); 7.50–7.43 (m, 8H, H_6, $H_{tpy\text{-}6}$); 7.25–7.17 (m, 8H, H_5, $H_{tpy\text{-}5}$); 5.28–5.12 (m, 14H, $H_{CD\text{-}1}$); 4.73 (s, 2H, S–CH_2–S); 3.82–3.08 (m, $H_{CD\text{-}2,\ CD\text{-}3,\ CD\text{-}4,\ CD\text{-}5,\ CD\text{-}6}$, CD_{CH3}).

^{13}C NMR (100 MHz, CD_3CN): δ in ppm 159.2, 158.7, 156.6, 155.9, 153.5, 149, 142.5, 139, 136.9, 129.7, 128.8, 128.5, 125.8, 125.5, 122.5, 98.9, 83.2, 82.7, 80.1, 79.9, 73.3, 72.5, 71.9, 70.6, 61.5, 59.2, 58.8, 35.1, 32.1, 30.3. ES-MS (+) m/z: 1454 $[M\text{-}3PF_6]^{+3}$.

Acknowledgements

Financial support from the Marie Curie Research Training Network grant "UNI-NANOCUPS" (MRTN-CT-2003-504233) is appreciated. P.B greatly acknowledges support via a Marie Curie Intra-European Fellowship (MEIF-CT-2005-515356) under the 6th European Community Framework Programme. We also wish to acknowledge COST-D31 action and the Aventis Foundation for support (MJJPS).

References

[1] Obeng, Y. S.; Bard, A. J. *Langmuir* **1991**, *7*, 195.
[2] Kim, Y. -T.; MacCarley, R. L.; Bard, A. J. *J. Phys. Chem.* **1992**, *96*, 7416.
[3] Otsuki, J.; Kameda, H.; Tomihira, S.; Sakaguchi, H.; Takido, T. *Chem. Lett.* **2002**, *6*, 610.
[4] Forster, R. J.; O Kelly, J. P. *J. Electrochem. Soc.* **2001**, *148*, E31.
[5] Bertoncello, P.; Kefalas, E.; Pikramenou, Z.; Unwin, P. R.; Forster, R. J. *J. Phys. Chem. B* **2006**, *110*, 10063.
[6] Will, G.; Nagaraja Rao, J. S. S.; Fitzmaurice, D. *J. Mater. Chem.* **1999**, *9*, 2297.
[7] Auditore, A.; Tuccitto, N.; Marzanni, G.; Quici, S.; Puntoriero, F.; Campagna, S.; Licciardello, A. *Chem. Comm.* **2003**, *19*, 2494.
[8] Maskus, M.; Abruna, H. D. *Langmuir* **1996**, *12*, 4455.
[9] Park, J.; Pasupathy, A. N.; Goldsmith, J. I.; Chang, C.; Yaish, Y.; Petta, J. R.; Rinkoski, M.; Sethna, J. P.; Abruna, H. D.; McEuen, P. L. *Nature* **2002**, 722.
[10] Park, J.; Pasupathy, A. N.; Goldsmith, J. I.; Soldatov, A. V.; Chang, C.; Yaish, Y.; Sethna, J. P.; Abruna, H. D.; Ralph, D. C.; McEuen, P. L. *Thin Solid Films* **2003**, *438*, 457.
[11] Figgemeier, E.; Constable, E. C.; Housecroft, C. E.; Zimmermann, Y. C. *Langmuir* **2004**, *20*, 9242.
[12] Haider, J. M.; Williams, R. M.; De Cola, L.; Pikramenou, Z. *Angew. Chem. Int. Ed.* **2003**, *42*, 1830.
[13] Haider, J. M.; Pikramenou, Z. *Eur. J. Inorg. Chem.* **2001**, 189.
[14] Pereira Silva, M. J. J.; Haider, J. M.; Heck, R.; Chavarot, M.; Marsura, A.; Pikramenou, Z. *Supramol. Chem.* **2003**, *15*, 563.
[15] Yang, Y. -W.; Chen, Y.; Liu, Y. *Inorg. Chem.* **2006**, *45*, 3014.
[16] Haider, J. M.; Pikramenou, Z. *Chem. Soc. Rev.* **2005**, *34*, 120.
[17] Nelissen, H. F. M.; Kercher, M.; De Cola, L.; Feiters, M. C.; Nolte, R. J. M. *Chem. Eur. J.* **2002**, *8*, 5407.
[18] Mortellaro, M. A.; Nocera, D. G. N. *J. Am. Chem. Soc.* **1996**, *118*, 7414.
[19] Li, C.; Fan, W.; Straus, D. A.; Leu, B.; Asano, S.; Zhang, D.; Han, J.; Meyyappan, M.; Zhou, C. *J. Am. Chem. Soc.* **2004**, *126*, 7750.
[20] Faiz, J.; Williams, R. M.; Pereira Silva, M. J. J.; Cola, L. D.; Pikramenou, Z. *J. Am. Chem. Soc.* **2006**, *128*, 4520.
[21] Faiz, J.; Spencer, N.; Pikramenou, Z. *Org. Biomol. Chem.* **2005**, *3*, 4239.
[22] Testaferri, L.; Tiecco, M.; Tingoli, M.; Chianelli, D.; Montanucci, M. *Synthesis* **1983**, *9*, 751.
[23] Katz, L.; Schroeder, W. *J. Org. Chem.* **1953**, *18*, 103.
[24] Tam, J. P.; Wu, C. R.; Liu, W.; Zhang, J. W. *J. Am. Chem. Soc.* **1991**, *113*, 6657.
[25] Wallace, T. J. *J. Am. Chem. Soc.* **1964**, *86*, 2018.
[26] Jeitler, J. R.; Turnbull, M. M.; Wikaira, J. L. *Inorg. Chim. Acta* **2003**, *351*, 331.
[27] Murguly, E.; Norsten, T. B.; Branda, N. *J. Chem. Soc., Perkin Trans. 2* **1999**, 2789.
[28] Anjali, K. S.; Vittal, J. J.; Dean, P. A. D. *Inorg. Chim. Acta* **2003**, *351*, 79.
[29] Gordon, A. J.; Ford, R. A. *The Chemist's Companion*; John Wiley & Sons: New York, 1972.
[30] Sauvage, J. P.; Collin, J. P.; Chambron, J. C.; Guillerez, S.; Coudret, C.; Balzani, V.; Barigelletti, F.; De Cola, L.; Flamigni, L. *Chem. Rev.* **1994**, *94*, 993.
[31] Maestri, M.; Armaroli, N.; Balzani, V.; Constable, E. C.; Cargill Thompson, A. M. W. *Inorg. Chem.* **1995**, *34*, 2759.
[32] Alcock, N. W.; Barker, P. R.; Haider, J. M.; Hannon, M. J.; Painting, C. L.; Pikramenou, Z.; Plummer, E. A. *J. Chem. Soc., Dalton Trans.* **2000**, *9*, 1447.
[33] Khramov, A. N.; Collinson, M. M. *Anal. Chem.* **2000**, *72*, 2943.
[34] Bard, A. J.; Faulkner, L. R. *Electrochemical Methods: Fundamentals and Applications*; 2nd Ed. Wiley: New York, 2001.
[35] Sheldrick, G. M. *Program Package for Crystal Structure Determination*; University of Gottingen: Germany, 1997.
[36] Demas, J. N.; Crosby, G. A. *J. Phys. Chem.* **1971**, *75*, 991.
[37] Nakamura, K. *Bull. Chem. Soc. Jpn.* **1982**, *55*, 2697.